

Effect of Radon Inhalation on Murine Brain Proteins: Investigation Using Proteomic and Multivariate Analyses

Shota Naoe^a, Ayumi Tanaka^a, Norie Kanzaki^b, Reiju Takenaka^a,
Akihiro Sakoda^b, Takaaki Miyaji^c, Kiyonori Yamaoka^d, and Takahiro Kataoka^{d*}

^aGraduate School of Health Sciences, Okayama University, ^dFaculty of Health Sciences,
Okayama University, Okayama 700-8558, Japan, ^bNingyo-toge Environmental Engineering Center,
Japan Atomic Energy Agency, Kagamino-cho, Okayama 708-0698, Japan,
^cAdvanced Science Research Center, Okayama University, Okayama 700-8530, Japan

Radon is a known risk factor for lung cancer; however, it can be used beneficially, such as in radon therapy. We have previously reported the enhancement of antioxidant effects associated with trace amounts of oxidative stress as one of the positive biological effects of radon inhalation. However, the biological effects of radon inhalation are incompletely understood, and more detailed and comprehensive studies are required. Although several studies have used proteomics to investigate the effects of radon inhalation on body proteins, none has focused on brain proteins. In this study, we evaluated the expression status of proteins in murine brains using proteomic and multivariate analyses to identify those whose expressions changed following two days of radon inhalation at a concentration of 1,500 Bq/m³. We found associations of radon inhalation with the expressions of seven proteins related to neurotransmission and heat shock. These proteins may be proposed as biomarkers indicative of radon inhalation. Although further studies are required to obtain the detailed biological significance of these protein alterations, this study contributes to the elucidation of the biological effects of radon inhalation as a low-dose radiation.

Key words: radon inhalation, proteomics, multivariate analysis, brain, oxidative stress

Radon inhalation is a recognized risk factor for lung cancer; however, it has also been used for clinical purposes, as in radon therapy [1]. We have previously reported that the positive mechanisms of action of radon inhalation include the enhancement of antioxidant [2] and anti-inflammatory [3] functions. For example, one day of radon inhalation at a concentration of 2,000 Bq/m³ was found to increase superoxide dismutase (SOD) activity and inhibit transient global cerebral ischemic injury [2]. Radon inhalation also suppresses lipopolysaccharide-induced inflammation by

suppressing inflammatory cytokines such as interleukin-6 [3]. However, the biological effects of radon inhalation on brain proteins remain unknown; other beneficial effects may be as yet undiscovered.

Proteomics is the large-scale study of proteins, with a focus on their structure and function. In proteomic analysis, a sample's complement of proteins are identified and their relative prevalences estimated by searching databases for matching peptide and fragment-ion mass spectra and sequences [4]. Based on liquid chromatography/tandem mass spectrometry (LC-MS/MS), proteomics is a powerful tool for biomedical research,

Received April 17, 2024; accepted June 27, 2024.

*Corresponding author. Phone: +81-86-235-7208; Fax: +81-86-235-7208
E-mail: kataokat@md.okayama-u.ac.jp (T. Kataoka)

Conflict of Interest Disclosures: No potential conflict of interest relevant to this article was reported.

and protein biomarker discovery has become one of its central applications [5]. Partial least-squares discriminant analysis (PLS-DA) is a commonly used analytical method for obtaining proteomic data [6]. PLS-DA is a supervised pattern recognition technique in which the variability of a dataset is correlated with class membership to provide an additional measure of confidence in the resulting clustering [7].

In the field of radiation biology, proteomics has resulted in the discovery of candidate biomarkers and further understanding of biological responses to ionizing radiation [8-10]; for example, the biological effects of X- [11, 12] and γ -rays [8, 13] have been studied using proteomic analysis. Several studies have used proteomics to investigate the effects of radon inhalation: for example, investigating biomarkers for lung cancer and injury associated with high concentrations or long-term radon exposure in human serum [14, 15] and rat lungs [16, 17]. However, no reports exist on the mouse brain. The brain is known to have low antioxidant capacity [18] and thus is considered to be susceptible to oxidative stress. We hypothesized that if we could use proteomic analysis and PLS-DA to identify proteins whose expressions fluctuate in the brain following low-dose radon inhalation, it might be useful to elucidate the effective clinical use of radon and its mechanisms of action.

Materials and Methods

Animals. BALB/c mice (8 weeks old, male) were obtained from Jackson Laboratory, Japan, Inc. Ethical approval for all study protocols were obtained from the Animal Care and Use Committee of Okayama University OKU-2021454. Mice were divided into two groups of six, housed under semi-daily light cycles and a temperature of $22 \pm 2^\circ\text{C}$, and given free access to food and water.

Radon exposure and sample preparation. After two days of environmental acclimation, the mice inhaled radon at $1,500 \text{ Bq/m}^3$ for two days. The source, exposure apparatus, and measurement of radon concentration in the cages were similar to those previously reported [2, 3]. Doll stones (Nigyotoge Genshiryoku Sangyo Co., Ltd., Tomata-gun, Okayama, Japan), which are natural minerals used as a source of radon gas in experimental settings, were placed in a vacuum desiccator, and naturally occurring radon gas was fed into

the mouse cages to equilibrate them at a constant concentration. To eliminate the influence of radon progenies, breeding cages were equipped with HEPA filters. A radon monitor (CRM-510, Femto-Tech Inc., OH, USA) was used to measure radon concentration. The control (Sham) group received air.

The animals were euthanized using CO_2 gas, and the brain and blood from the heart were obtained. After the blood rested for 30 min, serum was obtained using centrifugation at $563 \times g$ for 10 min at 4°C . Brains and serum were stored at -80°C until analysis.

LC-MS/MS analysis. Each brain was washed with 5 mL of SME buffer containing 300-mM sucrose, 10-mM 3-(*N*-morpholino)propanesulfonic acid-Tris (pH 7.0), 5-mM ethylenediaminetetraacetic acid, 10 $\mu\text{g/mL}$ leupeptin, 10 $\mu\text{g/mL}$ pepstatin A, and 0.5-mM dithiothreitol. The sample was homogenized with 7 mL of SME buffer while cooling on ice, and centrifuged at $193 \times g$ at 4°C for 10 min. The resulting supernatant was collected.

The supernatant was denatured with sodium dodecyl sulfate (SDS) at a final concentration of 1%, which was then incubated at 85°C for 10 min. The supernatant was collected using centrifugation at $14,900 \times g$ for 10 min and precipitated in 10% trifluoroacetic acid at -30°C for 30 min. The precipitate was collected by centrifugation at $14,900 \times g$ for 5 min and washed three times with 200 μL of washing solution (ethanol: diethyl ether = 1 : 1). The washed precipitate was briefly air-dried and reduced with 5-mM tris(2-carboxyethyl) phosphine (TCEP) in 50-mM ammonium bicarbonate buffer for 1 h at room temperature. The mixture was alkylated with 100-mM iodoacetamide in the dark for 1 h at room temperature, and precipitated in 10% trifluoroacetic acid at -30°C for 30 min. The precipitate was then collected by centrifugation at $14,900 \times g$ for 5 min and washed three times with 300 μL of washing solution. The washed precipitate was air-dried and dissolved in 20 μL of 50-mM ammonium bicarbonate buffer. Subsequently, trypsin was added to the protein at a mass ratio of 1/20, and the solution was incubated at 37°C for 24 h. Digested peptides were dried by evaporation and resuspended in buffer containing 0.1% formic acid 5% acetonitrile.

Proteomic analysis using LC-MS/MS was performed by the Department of Genomics and Proteomics, Advanced Science Research Center, Okayama University. Briefly, 1 μg of each sample was injected

into a liquid chromatography system (nanoElute; Bruker Japan, Inc., Yokohama, Japan) equipped with a Bruker TEN column (length, 100 mm; inner diameter, 75 μm ; particle size, 1.9 μm ; pore size, 120 \AA ; stationary phase, C18; mobile phases, (A) 0.1% formic acid in distilled water and (B) 0.1% formic acid in acetonitrile). The peptides were separated at 0.4 $\mu\text{L}/\text{min}$ and eluted from the column to the electrospray ionization/ion-trap mass spectrometer (amaZon ETD-OF; Bruker Japan) with the following gradient: 3-12% B for 49.5 min, 12-21% B for 22.5 min, 21-29% B for 10.8 min, 29-38% B for 7.2 min, 38-98% B for 5 min, and 98% B for 10 min. Cations were observed at a capillary voltage of 4.5 kV, ion trap uptake of 200,000 ions, and maximum ion uptake time of 200 ms. The top four peaks were measured in the mass ranges of 350-1,500 and 100-1,500 m/z in the MS and MS/MS scans, respectively.

Protein identification and quantification. A peak list was created from the MS/MS file, and database searches were performed using the Mascot Distiller ver 2.8.3 and the Mascot Server ver 2.8.2 (Matrix Science, K.K., Tokyo). All searches were performed using the UniProt database (UP589_M_musculus). To determine the false discovery rate (FDR), the database included targets and decoy, and the identification threshold was defined as the ratio of incorrect peptide spectrum matches (PSMs) to total PSM not exceeding 1% (hereafter referred to as Target FDR (+)). For trypsin cleavage, one missed cleavage was permitted. The fixed modification was carbamidomethylation of cysteine, and the variable modification was either no modification or the oxidation of methionine (hereafter referred to as Oxidation (M)). Peptide tolerance was set at ± 0.5 Da, MS/MS (fragment) tolerance at ± 0.5 Da, and peptide charges at 2+, 3+, and 4+. Each protein was identified based on the presence of one or more unique peptides. In addition, results without additional decoy databases for each search condition (hereafter referred to as Target FDR (-)) were obtained and compared to the Target FDR (+) results to search for false-positive peptides and proteins.

For each identified peptide, quantitative values or intensities were calculated based on the precursor peak areas using a Mascot Distiller. The threshold of correlation, which represents the degree of overlap between the theoretical and measured peak areas, and that of the fraction, which represents the ratio of the areas, were

not set. All samples were normalized by equalization of their total intensity, and the quantitative value for each protein was calculated as the sum of the intensities of the detected peptides.

Biochemical assays. SOD and catalase (CAT) activities, total glutathione (t-GSH) content, lipid peroxide (LPO) levels, and total protein levels in the brain were assayed using assay kits (SOD, Dojindo Molecular Technologies, Inc., Kumamoto, Japan; CAT, Cayman Chemical, MI, USA; t-GSH, OXIS Health Products, Inc., Portland, OR, USA; LPO, OXIS Health Products, Inc., Portland, OR, USA; total protein, Dojindo Molecular Technologies, Inc., Kumamoto, Japan). These were measured as previously described [3, 19].

Reactive oxygen metabolites (d-ROM) and biological antioxidant potential (BAP) tests in the serum were performed by Wismerll, Inc. (Tokyo). d-ROMs and BAP indicate the overall oxidative stress level and antioxidant capacity of the sample, respectively [20].

Statistical analyses.

1. Welch's *t*-test and Mann-Whitney test

Data on oxidative stress markers in the brain and serum are presented as means \pm standard errors of the mean (SEMs). The statistical significance of the differences was determined using Welch's *t*-tests. The Mann-Whitney test was performed to evaluate group differences in peptide and protein intensities obtained using the Mascot Distiller. Protein intensities that significantly differed were expressed as median ratios (radon inhalation group/Sham inhalation group or Rn/Sham). Differences among groups were considered statistically significant at $p < 0.05$.

2. Multivariate analysis

Regarding protein intensity, multivariate analysis was performed to further evaluate the effects of radon inhalation in ways other than by comparing the median values of the two groups. First, outliers were detected for each protein intensity based on the interquartile range (IQR), which is the difference between the first and third quartiles. Data exceeding a line 1.5 times the outer IQR from each of the first and third quartiles were considered outliers. Considering that variability affects PLS-DA [7], we aligned all samples with variables that did not contain outliers or missing values (138 proteins) in decreasing order of the *p*-values in the Mann-Whitney test. A total of 135 datasets containing the top 4, top 5 to all 138 proteins as variables were prepared. The smallest data set for which the PLS-DA perfor-

mance assessment described below could be performed contained four variables.

Each dataset was subjected to data normalization and PLS-DA using R-program-based MetaboAnalyst 6.0 [21]. Variables are shown as UniProt accessions, and data were normalized using auto-scaling (mean-centered and divided by the standard deviation of each variable). PLS-DA yields up to five latent variables (LV or Component) in each dataset, and 2-dimensional plots showing clusters of samples for the two primary LVs and variable-importance-in-projection (VIP) scores for each variable contributing to the LV were obtained.

Leave-one-out cross-validation (LOOCV) and permutation tests were performed to determine the optimal number of LVs for PLS-DA and to evaluate the model, respectively. In LOOCV, the models were fitted to all but one dataset and were compared to evaluate how they predicted the remaining data. This process was repeated until all the data were excluded once [22]. Thus, the accuracy, coefficient of determination of model fitting (R^2), and prediction (Q^2) in each case up to a maximum of five LVs were obtained, and the optimal number of LVs was predicted. Then, in the permutation test, the class assignments were permuted 1,000 times at the optimal number of LVs determined by LOOCV; thus, models were constructed. The sum of squares between/sum of squares within (B/W) rate was calculated for every class-assignment prediction. A histogram plotting these ratios is known as a distribution of random-class assignments. If the B/W ratio corresponding to the actual-class assignment is part of the distribution of the random-class assignments, the two clusters are not significantly classified [23]. Based on the permutation test results, we adopted models that resulted in statistically significant classifications.

Next, based on the VIP score for the component of interest in the model employed in the abovementioned methods, variables such as proteins with a VIP score > 1 contributed mainly to the component [24].

Results

Effects of different parameters on database search results. Several parameters can be established for a database search. The variable modification setting enables a database search that considers mass changes caused by the modification of amino acids. The disad-

vantages of this setting include increased search time and the possible loss of accuracy in identification; therefore, the most promising approach is to search with as few variable modification settings as possible [25]. Oxidation (M), a common variable modification, is recommended in most cases [26,27]. However, numerous spectra obtained from proteomic analysis can contain chemical or electrical noises resulting in false positives [28]. One method to avoid false positives and increase the reliability of the data is to adjust the identification threshold by evaluating the FDR using a decoy database. In this case, the identification threshold was adjusted to $< 1\%$ [28,29]. In addition, by comparing the data output using different search parameters, it is possible to find search parameters that render the data more reliable or to identify more false positives.

Comparing the results of Target FDR (–) and (+) searches under the same variable modification conditions, 32 (6) false-positive peptides (proteins) were identified when variable modification (none) and Target FDR (+) were set (Fig. 1A). Similarly, 35 (7) false-positive peptides (proteins) were detected in the Oxidation (M) and Target FDR (+) settings (Fig. 1B). The overlapping parts of the Venn diagrams do not include detectable false positives, and the peptides or proteins are reliable for the data (Fig. 1).

In the two searches for Target FDR (+), the FDR ($= 0.97$) was lower when Oxidation (M) was set, indicating that the identification threshold was more stringent (*i.e.*, the data were more reliable). In addition, despite the narrower identification threshold in the Oxidation (M) setting, a higher number of peptides and proteins, excluding false positives, were detected (Fig. 1). Therefore, we adopted the search results in the Oxidation (M) and Target FDR (+) settings, which yielded data for 2,627 peptides (370 proteins).

Effects of radon inhalation on the intensity of brain peptides and proteins. Of the 2,627 peptides detected, 707 showed oxidative modifications to methionine. Comparing the peptide intensities between groups, 19 showed significant increases or decreases (Table 1).

The intensities of 370 proteins were compared between groups, and significant changes were found in three proteins (Table 2). Radon inhalation significantly increased the intensity of cytoplasmic dynein 1 heavy chain 1 (DYNC1H1) and significantly decreased that of mitochondrial aspartate aminotransferase (AAT) and the kinesin-like protein KIF20B.

Further evaluation of the effect on protein expression using multivariate analysis. A total of 135 datasets were prepared for use in PLS-DA (Table 3 and 4). Table 4 shows the results of the LOOCV and permutation tests for the optimal number of LVs in each dataset. The accuracy and R² were left blank because Q² was negative for all LVs (1-5) in datasets including more

than 106 variables, and the optimal number of LVs was not determined. No permutation tests were performed on these datasets. The optimal number of LVs was determined for the other datasets; furthermore, datasets containing 6, 7, 9 and 11 variables were determined to be significant by permutation tests, and these datasets were adopted (Table 4). A value closer to 1 for

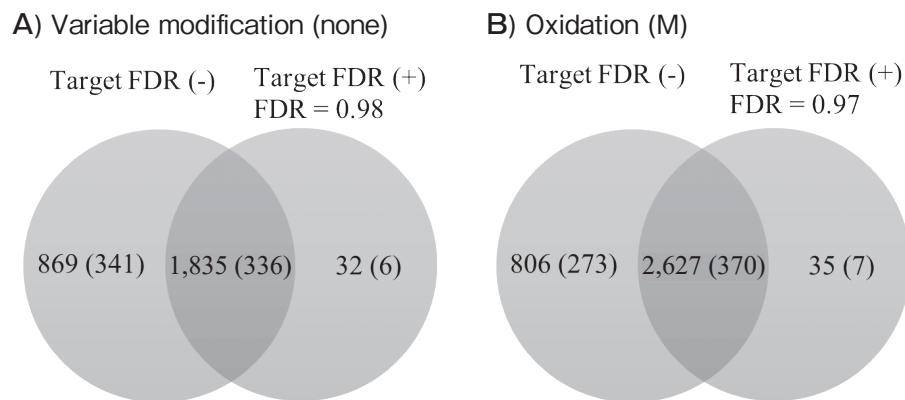


Fig. 1 Venn diagrams of the changes in the number of identified peptides and proteins with and without the adjustment for false discovery rate (FDR). Upper figure (A) shows the number of peptides (proteins) identified when no variable modification is set. Lower figure (B) shows the number of peptides (proteins) identified when the oxidative modification of methionine is set as a variable modification. Target FDR (+) is a setting that uses the decoy database to adjust the false discovery rate (FDR) so that it does not exceed 1%. Below that, the FDR in that case is shown.

Table 1 Effects of radon inhalation on the oxidation of methionine in certain proteins

Accession	Mass	z	Peptide sequence	Modifications	Intensity (median)		
					Sham	Rn	Ratio of Rn/Sham
P08553	95973	3	ATLEMVNHEK	(5) Oxidation (M)	4.6266 × 10 ⁵	9.8674 × 10 ⁵	2.1328 *
P32037	53957	2	GPAGVELNSMQPVK	(10) Oxidation (M)	5.8263 × 10 ⁵	1.0834 × 10 ⁶	1.8596 *
Q8K2B3	73623	2	SMTLEIR	(2) Oxidation (M)	5.9568 × 10 ⁵	1.1015 × 10 ⁶	1.8492 *
P08752	41033	2	MFDVGGQR	(1) Oxidation (M)	1.7242 × 10 ⁶	2.8606 × 10 ⁶	1.6591 *
B2RSH2	40905	2	MFDVGGQR	(1) Oxidation (M)	1.7242 × 10 ⁶	2.8606 × 10 ⁶	1.6591 *
P97427	62471	2	MDENQFVAVTSTNAAK	(1) Oxidation (M)	5.8605 × 10 ⁶	7.0749 × 10 ⁶	1.2072 *
E9PWE8	74294	2	MDENQFVAVTSTNAAK	(1) Oxidation (M)	5.8605 × 10 ⁶	7.0749 × 10 ⁶	1.2072 *
Q03265	59830	2	TGTAEMSSILEER	(6) Oxidation (M)	7.3952 × 10 ⁶	6.5768 × 10 ⁶	0.88934 *
A0A0A0MQF6	38914	3	VIIISAPSADAPMFVGVNHEK	(12) Oxidation (M), (15) Oxidation (M)	3.8324 × 10 ⁷	3.2167 × 10 ⁷	0.83933 *
Q7TMM9	50274	2	EVDEQMLNVQNK	(6) Oxidation (M)	1.4219 × 10 ⁷	1.1719 × 10 ⁷	0.82421 *
Q9CWF2	50377	2	EVDEQMLNVQNK	(6) Oxidation (M)	1.4219 × 10 ⁷	1.1719 × 10 ⁷	0.82421 *
P68372	50255	2	EVDEQMLNVQNK	(6) Oxidation (M)	1.4219 × 10 ⁷	1.1719 × 10 ⁷	0.82421 *
P99024	50095	2	EVDEQMLNVQNK	(6) Oxidation (M)	1.4219 × 10 ⁷	1.1719 × 10 ⁷	0.82421 *
P40142	68272	3	NMAEQIQEIYSQVQSK	(2) Oxidation (M)	1.8551 × 10 ⁶	1.5048 × 10 ⁶	0.81121 *
A0A0A6YW88	52042	2	LMEVEQDQR	(2) Oxidation (M)	8.4640 × 10 ⁵	6.4776 × 10 ⁵	0.76531 *
P62814	56857	3	GPVVLAEFLDIMGQPINPQCR	(13) Oxidation (M)	1.7331 × 10 ⁶	9.8976 × 10 ⁵	0.57110 *
P56480	56265	3	IMDPNIVGNEHYDVAR	(2) Oxidation (M)	5.1591 × 10 ⁶	2.0215 × 10 ⁶	0.39183 *
P56564	59755	3	MLQMLVPLIISSLVTGMAALDSK	(4) Oxidation (M), (18) Oxidation (M)	1.4991 × 10 ⁵	4.9408 × 10 ⁴	0.32958 *
Q8C2Q8	30294	2	MTAMDNASK	(1) Oxidation (M), (4) Oxidation (M)	1.2267 × 10 ⁵	1.9432 × 10 ⁴	0.15840 *

The Table shows the UniProt accession and mass of the protein, the charge of the identified peptide, the amino acid sequence, information on modifications, and peptide intensity. Peptide intensities are presented as median values and median ratios of the radon inhalation group to the control group. Each study group comprised six mice. *P<0.05

Table 2 Effects of radon inhalation on protein expression levels

Accession	Proteins	Intensity (median)		
		Sham	Rn	Ratio of Rn/Sham
Q9JHU4	Cytoplasmic dynein 1 heavy chain 1	1.6777×10^7	2.0426×10^7	1.2175 *
P05202	Mitochondrial aspartate aminotransferase	1.7809×10^7	1.5424×10^7	0.86608 *
Q80WE4-4	Kinesin-like protein KIF20B	7.0934×10^5	4.9000×10^5	0.69079 *

The Table shows the proteins whose intensities were significantly altered by radon inhalation. Protein intensities are presented as median values and median ratios of the radon inhalation group to the control group. Each study group comprised six mice. * $P < 0.05$

Table 3 Variables for PLS-DA aligned in decreasing order of *P* value in the Mann-Whitney tests. Variables are shown as UniProt accessions

Accession	<i>P</i> -value in Mann-Whitney test	Accession	<i>P</i> -value in Mann-Whitney test	Accession	<i>P</i> -value in Mann-Whitney test
P05202	0.02500	A0A338P769	0.3367	E9QKR0	0.7488
Q80WE4-4	0.03740	F6QPR1	0.3367	Q01853	0.7488
P43006-2	0.05470	E9PWE8	0.4233	O08749	0.7488
P63260	0.07820	A3KGU9	0.4233	P63328	0.7488
P39053-4	0.07820	P17427	0.4233	P31650	0.7488
B2RXT3	0.07820	Q9CR68	0.4233	P35700	0.7488
Q3U2G2	0.07820	Q8CAQ8-5	0.4233	Q6P1F6	0.7488
P04370-4	0.1093	P11404	0.4233	Q8K596-2	0.7488
Q8C605	0.1093	Q792Z1	0.4233	D3YVF0	0.7488
Q9CZU6	0.1093	S4R2F3	0.4233	Q9Z2W9	0.7488
B2M1R6	0.1093	Q9QUI0	0.4233	P62812	0.7488
Q7M6Y3	0.1093	Q9CZ30	0.4233	Q3UX10	0.8728
Q8BGH2	0.1093	P52480-2	0.5218	P05063	0.8728
Q60737	0.1093	P84084	0.5218	P26443	0.8728
O35633	0.1495	P15105	0.5218	A0A0A6YY91	0.8728
Q8C266	0.1495	P62874	0.5218	E9Q1G8	0.8728
P62835	0.1495	G5E902	0.5218	Q8BG39	0.8728
P28652	0.2002	E9PV63	0.5218	Q9D051	0.8728
P62814	0.2002	Q9D0K2	0.5218	P14211	0.8728
Q8VED5	0.2002	P40124	0.5218	K4DI76	0.8728
P31648	0.2002	Q9D8N0	0.5218	P00397	0.8728
P58252	0.2002	Q3UY21	0.5218	Q9CY14	0.8728
P06745	0.2002	Q4KMM3	0.5218	Q8K0S0	0.8728
P63005	0.2002	Q62277	0.5218	Q9CZC8	0.8728
P68033	0.2623	P62746	0.5218	P14231	0.8728
P16330	0.2623	A0A2I3BQS2	0.5218	D3YWF6	0.8728
P61922	0.2623	O08539	0.5218	Q9CQC3	0.8728
Q02053	0.2623	Q52KG9	0.5218	Q3U4W8	0.8728
Q61644	0.2623	P52480	0.6310	A0A0G2JGS4	1.0000
Q9DBG3	0.2623	P11798	0.6310	A0A494B945	1.0000
E9Q0H6	0.2623	Q3UHH0	0.6310	J3QMG3	1.0000
Q9Z1S5	0.2623	A2ALL9	0.6310	O35544	1.0000
P42669	0.2623	Q9CZ13	0.6310	P08752	1.0000
Q9CVB6	0.2623	Q9R1T4	0.6310	P18760	1.0000
Q05816	0.2623	Q9JIS5	0.6310	Q99PT1	1.0000
Q99P72	0.2623	P30275	0.6310	A2AQR0	1.0000
P62881-2	0.2623	O88569-2	0.6310	P17742	1.0000
P68369	0.3367	P62259	0.6310	Q91VD9	1.0000
P61205	0.3367	Q3TLP8	0.6310	P47708	1.0000
Q68FG2	0.3367	Q9CQQ7	0.6310	H3BK84	1.0000
K3W4T3	0.3367	D3Z7P3	0.6310	P63321	1.0000
P35486	0.3367	Q9DB41	0.6310	Q3UH59	1.0000
Q7TSJ2	0.3367	D3Z4K0	0.6310	Q9DBJ1	1.0000
Q8BMF4	0.3367	Q8R5H6	0.6310	P28651	1.0000
Q80SW1	0.3367	Q8BFZ3	0.7488		
Q61792	0.3367	Q04447	0.7488		
Q9EQF6	0.3367	P05064	0.7488		

Table 4 LOOCV and permutation tests for each dataset

Number of variables	LOOCV			Permutation test	
	Number of LVs	Accuracy	R ²	Q ²	P-value
1	-	-	-	-	-
2	-	-	-	-	-
3	-	-	-	-	-
4	1	0.75	0.64174	0.48283	0.108
5	1	0.91667	0.69296	0.51297	0.076
6	1	0.83333	0.71308	0.5444	0.014*
7	1	0.83333	0.69023	0.51292	0.021*
8	1	0.91667	0.68864	0.50862	0.131
9	1	0.91667	0.74109	0.5538	0.037*
10	1	0.91667	0.74655	0.57222	0.051
11	1	0.91667	0.73378	0.53553	0.048*
12	1	0.91667	0.73174	0.53795	0.055
13	1	0.91667	0.70813	0.49176	0.067
14	1	0.91667	0.74838	0.5547	0.095
15	1	1.0	0.72653	0.52151	0.097
16	1	1.0	0.74628	0.54157	0.089
17	1	1.0	0.72853	0.50609	0.100
18	1	1.0	0.74248	0.51222	0.138
19	1	0.91667	0.73512	0.49659	0.115
20	1	0.83333	0.73842	0.48813	0.127
21	1	0.91667	0.74017	0.49331	0.152
22	1	0.91667	0.73436	0.47495	0.160
23	1	0.91667	0.74401	0.48568	0.186
24	1	0.91667	0.7592	0.49137	0.161
25	1	0.91667	0.75966	0.48564	0.174
26	1	1.0	0.77581	0.50924	0.189
27	1	0.91667	0.78418	0.5112	0.177
28	1	0.91667	0.79972	0.51919	0.236
29	1	0.91667	0.78308	0.49743	0.232
30	1	0.83333	0.77959	0.48929	0.232
31	1	0.91667	0.77021	0.47391	0.240
32	1	0.91667	0.77316	0.47134	0.277
33	1	1.0	0.78735	0.48907	0.293
34	1	0.91667	0.79012	0.48263	0.279
35	1	1.0	0.79455	0.48424	0.303
36	1	1.0	0.8026	0.48851	0.309
37	1	1.0	0.79364	0.47217	0.313
38	1	1.0	0.80293	0.47048	0.275
39	1	1.0	0.82027	0.4887	0.324
40	1	1.0	0.82764	0.49257	0.411
41	1	1.0	0.84428	0.5023	0.411
42	1	1.0	0.83668	0.49222	0.446
43	1	0.91667	0.83166	0.48076	0.403
44	1	0.91667	0.84319	0.4976	0.452
45	1	0.91667	0.84194	0.48623	0.424
46	1	0.91667	0.84175	0.4915	0.418
47	1	0.83333	0.83509	0.47478	0.417
48	2	0.91667	0.94302	0.4807	0.991
49	2	0.91667	0.9421	0.47318	0.987
50	2	0.91667	0.94504	0.4574	0.992
51	2	0.83333	0.94454	0.48209	0.990
52	2	0.83333	0.94405	0.45941	0.995
53	2	0.83333	0.94206	0.4503	0.999
54	2	0.83333	0.94174	0.4483	0.987
55	2	0.83333	0.94127	0.4455	0.990
56	2	0.91667	0.93692	0.43929	0.989
57	2	0.91667	0.93506	0.43822	0.994
58	2	0.83333	0.93175	0.42131	0.998
59	2	0.83333	0.93207	0.40073	1.000
60	2	0.91667	0.92961	0.39207	0.995
61	2	0.91667	0.93504	0.40725	0.999
62	2	0.91667	0.93408	0.39398	0.995
63	2	0.91667	0.93113	0.38928	0.986
64	2	0.83333	0.92978	0.37334	0.995
65	2	0.83333	0.92852	0.35337	0.996
66	2	0.75	0.92866	0.34548	1.000
67	2	0.83333	0.93029	0.32773	1.000
68	2	0.75	0.92966	0.32544	1.000
69	2	0.75	0.92917	0.31454	1.000

Number of variables	LOOCV			Permutation test	
	Number of LVs	Accuracy	R ²	Q ²	P-value
70	2	0.75	0.9285	0.29643	1.000
71	2	0.75	0.92871	0.275	1.000
72	2	0.75	0.9283	0.25398	1.000
73	2	0.83333	0.92923	0.28364	1.000
74	2	0.66667	0.92796	0.27117	0.998
75	2	0.66667	0.92996	0.27819	0.998
76	2	0.66667	0.92843	0.26863	0.996
77	2	0.75	0.92675	0.27346	0.996
78	2	0.58333	0.92744	0.25314	0.997
79	2	0.58333	0.78816	0.16878	0.999
80	2	0.58333	0.92521	0.2272	0.994
81	2	0.58333	0.92515	0.20274	0.995
82	2	0.58333	0.92439	0.19259	0.993
83	2	0.58333	0.91938	0.18764	0.996
84	2	0.5	0.9901	0.097976	0.996
85	2	0.58333	0.92372	0.18736	0.996
86	2	0.58333	0.92149	0.18358	0.995
87	2	0.58333	0.92155	0.16529	0.994
88	3	0.66667	0.99061	0.2007	1.000
89	3	0.5	0.99058	0.19033	1.000
90	4	0.75	0.95936	0.20102	0.942
91	2	0.58333	0.93357	0.14824	1.000
92	2	0.58333	0.93239	0.15196	1.000
93	2	0.58333	0.93181	0.13438	1.000
94	2	0.5	0.93177	0.12906	1.000
95	2	0.5	0.93288	0.13458	1.000
96	2	0.5	0.93395	0.12374	1.000
97	2	0.5	0.93557	0.10886	1.000
98	2	0.5	0.93609	0.096212	1.000
99	2	0.5	0.93576	0.080379	1.000
100	2	0.5	0.93535	0.062826	1.000
101	2	0.5	0.93337	0.0461	1.000
102	2	0.5	0.98817	0.0084149	1.000
103	2	0.5	0.93154	0.019586	1.000
104	2	0.5	0.93388	0.024747	1.000
105	2	0.5	0.93396	0.0034757	1.000
106	-	-	-	0<	-
107	-	-	-	0<	-
108	-	-	-	0<	-
109	-	-	-	0<	-
110	-	-	-	0<	-
111	-	-	-	0<	-
112	-	-	-	0<	-
113	-	-	-	0<	-
114	-	-	-	0<	-
115	-	-	-	0<	-
116	-	-	-	0<	-
117	-	-	-	0<	-
118	-	-	-	0<	-
119	-	-	-	0<	-
120	-	-	-	0<	-
121	-	-	-	0<	-
122	-	-	-	0<	-
123	-	-	-	0<	-
124	-	-	-	0<	-
125	-	-	-	0<	-
126	-	-	-	0<	-
127	-	-	-	0<	-
128	-	-	-	0<	-
129	-	-	-	0<	-
130	-	-	-	0<	-
131	-	-	-	0<	-
132	-	-	-	0<	-
133	-	-	-	0<	-
134	-	-	-	0<	-
135	-	-	-	0<	-
136	-	-	-	0<	-
137	-	-	-	0<	-
138	-	-	-	0<	-

The Table shows the results of the leave-one-out cross-validation (LOOCV) and permutation tests for each dataset containing between 4 and 138 variables. The LOOCV provided the accuracy, coefficient of determination of model fitting (R²) and prediction (Q²), and optimal number of latent variables (LVs) for each model. The permutation test was used to assess whether statistically significant classifications were obtained. *P<0.05

R^2 indicates that the model has a good fit, and a value closer to 1 for Q^2 indicates that the model has good predictive performance [30]. Although there is no general threshold for Q^2 that implies a good prediction [31], a model may be considered good if R^2 and Q^2 are >0.5 [30,32]. Therefore, the models in the datasets we adopted would be acceptable.

In the PLS-DA model, each cluster in the sham and radon-inhalation groups partially overlapped but was separated by component 1, because the optimal number of LVs was 1 (Fig. 2). Two to six variables that satisfied VIP scores >1 were thought to contribute to com-

ponent 1 (Table 5). These were excitatory amino acid transporter 2 (EAAT2), KIF20B, heat shock 70 kDa protein 4 (HSPA4), myelin basic protein (MBP), dynamin-1 (DNM1), and AAT (Table 6).

Effects of radon inhalation on oxidative stress in the brain and serum. Radon inhalation significantly decreased t-GSH content and SOD and CAT activities and increased LPO levels in the brain; however, none of these changes were significant. In addition, changes in the d-ROM and BAP levels in the serum were negligible (Fig.3).

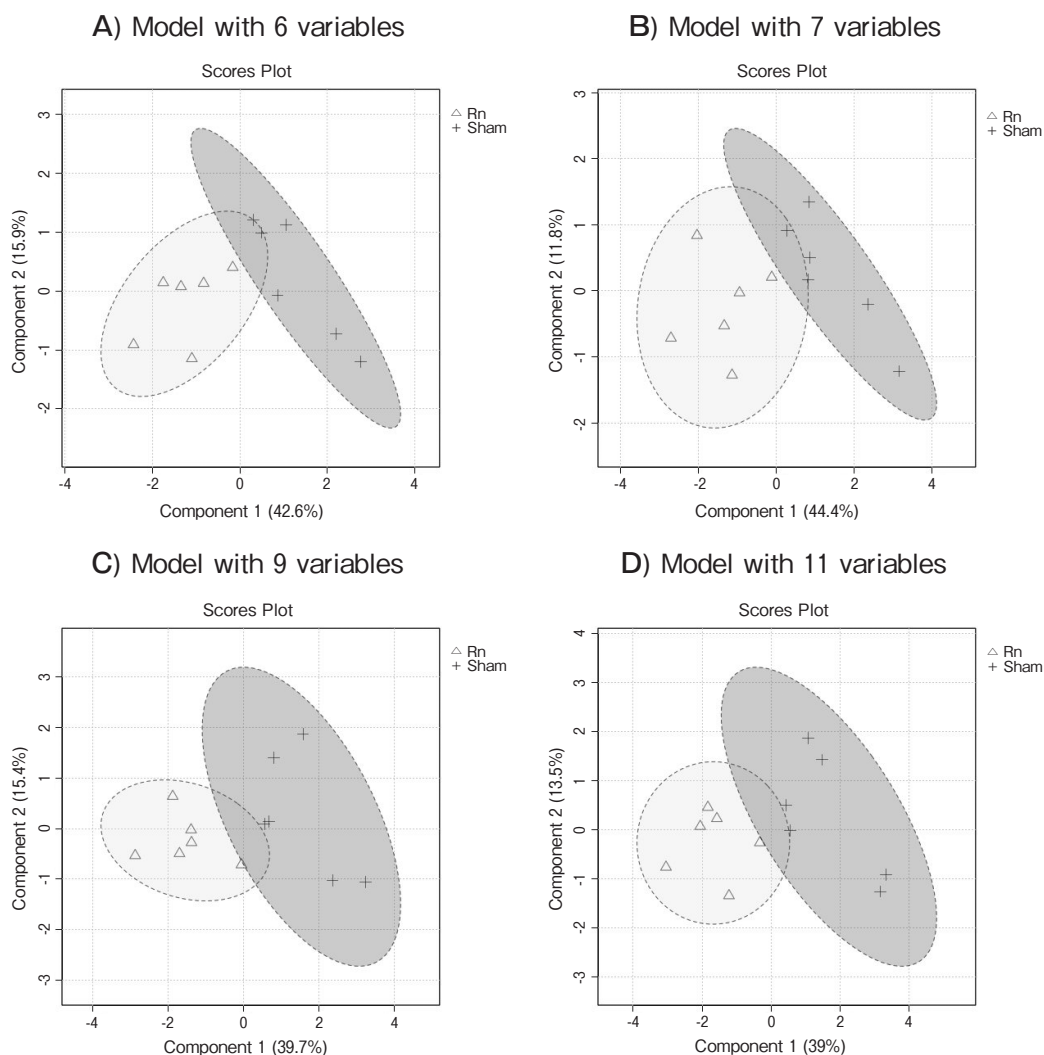


Fig. 2 Score plots showing clusters of samples for components 1 and 2 obtained using PLS-DA for datasets including six **A**), seven **B**), nine **C**), and eleven **D**) variables. Cross plots indicate the control group and triangular plots the radon inhalation group. The figure shows a scatter plot of the two components with the main variation, with the values in brackets on each axis indicating the percentage of variation contained in each component out of the total variation. They were modelled using the MetaboAnalyst 6.0 program.

Table 5 Variables with a VIP score >1 in each model adopted

Number of variables	Number of LVs	Variables with a VIP score >1
6	1	P43006-2, Q80WE4-4
7	1	P43006-2, Q80WE4-4, Q3U2G2
9	1	P43006-2, Q80WE4-4, Q3U2G2, P04370-4, P39053-4, P05202
11	1	P43006-2, Q80WE4-4, Q3U2G2, P04370-4, P39053-4, P05202

Variables with a variable importance in projection (VIP) score >1 for the main LV in each model were determined to contribute strongly to group separation. The Table shows proteins with a VIP score >1 that contributed to the LV in each of the successful models

Table 6 Correspondence between accession and protein

Accession	Proteins
P43006-2	Excitatory amino acid transporter 2
Q80WE4-4	Kinesin-like protein KIF20B
Q3U2G2	Heat shock 70kDa protein 4
P04370-4	Myelin basic protein
P39053-4	Dynamin-1
P05202	Mitochondrial aspartate aminotransferase

Discussion

While long-term radon exposure creates a lung cancer risk, short-term radon can have a positive effect on pain disorders. Positive effects have also been observed for certain radon spa baths, and radon is now used for health purposes [1]. We previously reported that short-term radon inhalation in rodents contributes to the suppression of symptoms of various diseases, and the mechanism of action includes the enhancement of antioxidant and anti-inflammatory effects due to trace amounts of oxidative stress [2,3,33]. However, the biological effects of short-term radon inhalation are incompletely understood, and more detailed and comprehensive studies are required. In the present study, we evaluated the state of protein expression in the brain following two days of radon gas inhalation at a concentration of 1,500 Bq/m³, an exposure condition similar to that used therapeutically.

The proteomic analysis performed in this study did not use derivatives or other materials to analyze specific proteins [4], and it was not aimed at the structural analysis of amino acids or peptides. Therefore, it was difficult to interpret the expression trends of specific peptides or proteins when determining the appropriate database search parameters, particularly variable modifications. Regarding comprehensiveness, we consid-

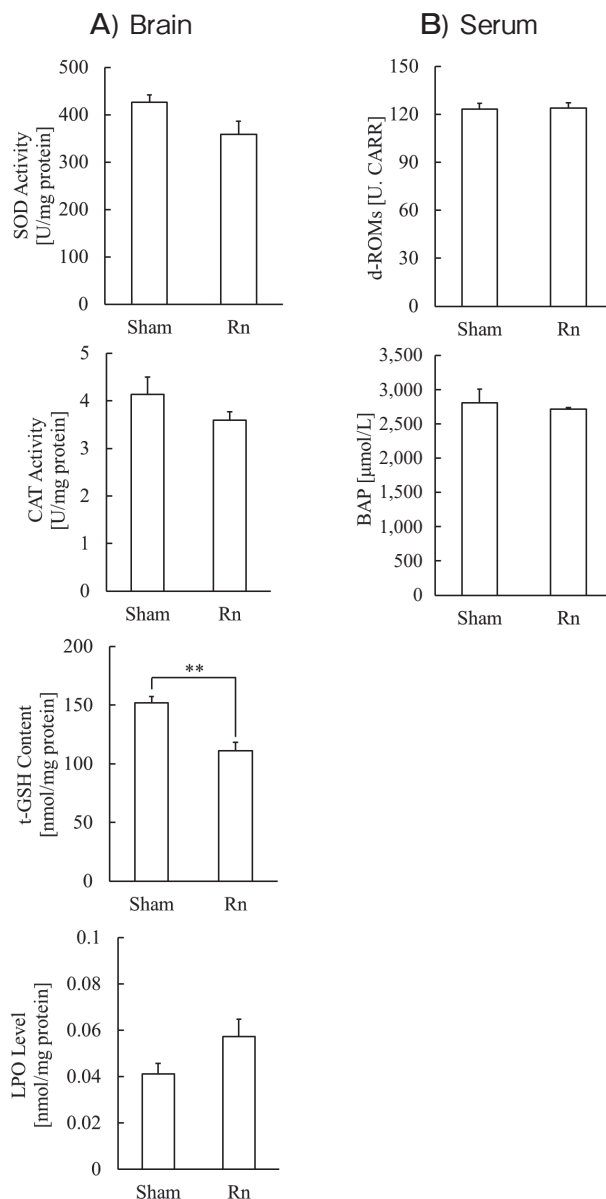


Fig. 3 Effects of radon inhalation on oxidative stress markers in the brain **A)** and serum **B)**. Data are presented as means ± SEMs. Each study group comprised five or six mice. **P*<0.05.

ered search parameters that would increase the number of detections while ensuring data quality. Consequently, Oxidation (M) and Target FDR (+) conditions were considered optimal. The data obtained using this method included peptides with oxidative methionine modifications. Peptide intensities were compared between the groups, and some were significantly increased or decreased by radon inhalation. This suggests that radon inhalation significantly affects the oxidative modification of methionine. However, these results were obtained in a secondary manner, and we were unable to clarify how the changes in peptide intensity, including the oxidative modification of methionine caused by radon inhalation, are related to protein activity and associated biological effects. Methionine residues are particularly susceptible to oxidation via ROS, which results in the formation of R- or S-stereoisomers of methionine sulfoxide (MetO). The MetO content of proteins increases with age, as more ROS are generated and antioxidant capacity decreases. Indeed, the expression of stereospecific methionine sulfoxide reductases (Msrs), which reduce MetO residues, results in life span extensions [34]. These findings suggest that oxidative stimulation associated with radon inhalation may significantly reduce MetO levels in proteins and prolong their lifespan. Future clarification of the effects of radon inhalation on MetO and Msr levels and lifespan is expected.

The proteins used in the PLS-DA were not selected for any function. Most of the proteins detected in this study were unreported in studies on short-time radon inhalation. For the sake of comprehensiveness, we wanted to use as many variables as possible, so the datasets were prepared with a focus on statistics. We also did not determine the best model for the four PLS-DA models we adopted. This was because each model had common variables with a VIP score > 1, and the highlighted proteins in the model including 11 variables covered those in the other models.

For reference, we describe the results of the smoothed receiver-operating-characteristic curve analysis for the six proteins with a VIP score > 1. Their area under the curves (AUCs) were 0.8115 for EAAT2, 0.7879 for KIF20B, 0.7805 for HSPA4, 0.7647 for MBP, 0.7714 for DNMI1, and 0.8450 for AAT. AUC values are assessed as follows: 0.9–1.0 = excellent; 0.8–0.9 = good; 0.7–0.8 = fair; 0.6–0.7 = poor; 0.5–0.6 = failure [35]. According to this, the AUCs of the six proteins would

be assessed as good or fair.

Proteomic analysis revealed that DYNCIH1, AAT, and KIF20B, which showed significant changes in protein intensity between groups, may be proteins that are characteristically altered in the brain following radon inhalation. Furthermore, EAAT2, HSPA4, MBP, and DNMI1, which were also identified using PLS-DA, may also be indicators affected by radon inhalation. However, determining whether these indicators increased or decreased after radon inhalation was impossible.

Both cytoplasmic dynein and kinesin are cytoskeletal (microtubule) motors that function in neuronal polarization, elongation, shape, and neurotransmission. These proteins are responsible for the transport of various cargo, such as receptor subunits, organelles, proteins, and RNA, and their dysfunction is associated with several neurological diseases [36,37]. DYNCIH1 is essential for the normal functioning of the nervous system, and mutations in this protein can cause neurodegenerative disorders [38]. KIF20B is a kinesin-6 family member and a key player in dedifferentiation, which is a critical step in cytoplasmic division. The knockout of KIF20B in human cycling cells results in the inability of cells to divide in the late stages of cytoplasmic division [36]. AAT is a catalyst that is highly active in both the mitochondria and cytoplasm and plays a key role in both the synthesis and oxidation of glutamate [39]. Glutamate is the major excitatory neurotransmitter in the brain, and the overproduction of glutamate at the synapse or inhibition of its reuptake from the synaptic cleft results in toxicity to adjacent neurons. Glutamate excitotoxicity may play a prominent pathophysiological role in severe acute disorders, such as stroke and epilepsy, and is a prominent factor in slowly progressive neurodegenerative diseases, such as amyotrophic lateral sclerosis (ALS) and Parkinson's disease. To prevent excitotoxicity, it is critical to maintain low levels of extracellular glutamate [40]. EAAT2 is a glutamate transporter responsible for 90% of total glutamate uptake. Glutamate transporters tightly regulate glutamate concentration in the synaptic cleft, and dysfunction of EAAT2 has been implicated in the development of neurodegenerative diseases, including Alzheimer's disease (AD) and ALS [41]. Heat-shock proteins (HSPs) are induced by stress denaturation and participate in protection against various disorders, including stroke and epilepsy [42]. HSPA4, a member of the HSP110 family, functions as a nucleotide exchange factor for the

HSP70 chaperone and is involved in protein quality control, proper protein folding, and homeostasis [43]. HSPA4 has also been reported as a potential target for therapeutic drug development in neurodegenerative diseases [44]. MBP is a major component of myelin, which forms an insulating sheath around nerve axons in the central nervous system, allowing efficient signal transduction; damage to myelin sheaths is the key characteristic of multiple sclerosis [45,46]. Dynamins are GTPases associated with diverse cellular processes, including release of transport vesicles, mitochondrial fusion and fission, chloroplast and peroxisome division, cell division and resistance to viral infection [47]. The dynamin DNMI is known to have a role in clathrin-mediated endocytosis and neurotransmitter release into the synaptic cleft and has been suggested to be involved in memory formation and epileptic encephalopathy [48,49].

As described above, radon inhalation may modulate the neurotransmitter system because it affects the expressions of DYNC1H1, AAT, KIF20B, EAAT2, HSPA4, MBP, and DNMI, which play important roles in neurotransmission and neurodegenerative diseases. However, the biological significance of changes in protein intensity could not be clarified in this study. Low-dose ionizing radiation has recently gained significant support from both clinicians and researchers as a therapeutic modality for AD [50]. Moreover, it has been reported that when rats are exposed to a sauna using radon water with a water concentration of 37 Bq/m³ for 20 min once a day for 10 days, epileptic symptoms are improved by inhibiting oxidative stress [51]. The indications for radon therapy currently do not include neurodegenerative diseases [1]. In addition to the above findings, the results of this study may result in the proposal of new uses for radon therapy; however, further research is required.

Next, we discussed the effects of oxidative stress under the conditions used in this experiment. In our previous studies, an inhalation of 1,000 Bq/m³ radon for 1 day or 2,000 Bq/m³ radon for 0.5, 1, or 2 day increased SOD activity in the mouse brain, whereas inhalation of 1,000 Bq/m³ for 2 or 4 day resulted in control levels [2,52]. The absorbed dose in the mouse brain under these inhalation conditions was approximately 75-300 nGy [53]. Although SOD activity is important for determining the redox status of organs with low antioxidant capacity, such as the brain [18], it

is unlikely that a negative effect on SOD activity in the brain would appear in this dose range. In the present study, a slight decrease in SOD activity was observed under inhalation conditions and an estimated absorbed dose to the brain of 225 nGy [53]. Furthermore, t-GSH content was significantly decreased, and LPO levels were slightly increased, indicating that radon inhalation did not enhance antioxidant activity. However, because oxidative stress is mediated by the serum, the degree of oxidative damage caused by radon may have been minimal under the inhalation conditions used in the present study. Although we did not obtain data for the same estimated absorbed dose or for different inhalation durations at a concentration of 1,500 Bq/m³, our findings suggest that the effects of radon inhalation may change with minor changes in the inhalation conditions. This may also be true of the effects on protein expression. In the future, it will be necessary to clarify the characteristics of changes in oxidative effects in response to radon concentration and the duration of inhalation.

This study had several limitations. First, the effects of radon inhalation on proteins were examined in the brain as a whole, but not in different parts of the brain, so it was impossible to evaluate the effects on protein expression there. Second, quantitative proteomic analysis using stable isotope labeling [54] was not performed; therefore, our results were not as reliable as with that type of analysis. In addition, considering the low number of samples and high variability, we cannot refer only to the effects of inhalation in this study. An increase in the number of samples, mRNA-based evaluations, and absolute quantification, such as western blotting of each protein, are necessary. Third, because we wanted to use the intensities of many peptides, we did not set correlation and fraction thresholds as quality assurance. Doing so would have reduced the number of available data but could have ensured greater validity of quantitative values. Fourth, it was not within the scope of this paper to determine the biological significance of the effects on each protein. We considered that the first mechanism of action of various responses after radon inhalation is the generation of ROS, and the same is true for protein expression. However, we could not elucidate the mechanistic pathway to this response, and further clarification is desirable. Finally, the present results are only applicable to normal mice brains; the effects in other organs or disease-model mice may differ.

In conclusion, the present study suggests that radon inhalation in mice at a concentration of 1,500 Bq/m³ for two days may alter the expressions of DYNC1H1, AAT, KIF20B, EAAT2, HSPA4, MBP, and DNMT1 in the brain. These proteins, related to neurotransmission and HSPs, may be proposed as biomarkers whose expression is characteristically altered in the brain by short-term radon inhalation. In addition, radon inhalation may have a pronounced effect on the oxidative modification of methionine. However, further studies are required to obtain detailed insights into the effects of individual indicators. This study contributes to the elucidation of the biological effects of radon inhalation as a form of low-dose radiation therapy.

Acknowledgments. The authors are grateful to Mr. Keita Tateno and Ms. Ikuyo Sugimoto at the Department of Genomics and Proteomics, Advanced Science Research Center, Okayama University for their technical support.

References

- Maier A, Wiedemann J, Rapp F, Papenfuß F, Rödel F, Hehlhans S, Gaipl US, Kraft G, Fournier C and Frey B: Radon Exposure-Therapeutic Effect and Cancer Risk. *Int J Mol Sci* (2021) 22: 316.
- Kataoka T, Etani R, Takata Y, Nishiyama Y, Kawabe A, Kumashiro M, Taguchi T and Yamaoka K: Radon inhalation protects against transient global cerebral ischemic injury in gerbils. *Inflammation* (2014) 37: 1675–1682.
- Kataoka T, Naoe S, Murakami K, Fujimoto Y, Yukimine R, Tanaka A and Yamaoka K: Immunomodulatory Effects of Radon Inhalation on Lipopolysaccharide-Induced Inflammation in Mice. *Int J Environ Res Public Health* (2022) 19: 10632.
- Butterfield DA, Perluigi M and Sultana R: Oxidative stress in Alzheimer's disease brain: new insights from redox proteomics. *Eur J Pharmacol* (2006) 545: 39–50.
- Hu S, Loo JA and Wong DT: Human body fluid proteome analysis. *Proteomics* (2006) 6: 6326–6353.
- Saccenti E and Timmerman ME: Approaches to Sample Size Determination for Multivariate Data: Applications to PCA and PLS-DA of Omics Data. *J Proteome Res* (2016) 15: 2379–2393.
- Karp NA, Griffin JL and Lilley KS: Application of partial least squares discriminant analysis to two-dimensional difference gel studies in expression proteomics. *Proteomics* (2005) 5: 81–90.
- Bakshi MV, Azimzadeh O, Merl-Pham J, Verreet T, Hauck SM, Benotmane MA, Atkinson MJ and Tapio S: In-Utero Low-Dose Irradiation Leads to Persistent Alterations in the Mouse Heart Proteome. *PLoS ONE* (2016) 11: e0156952.
- Yamaguchi M, Tataru Y, Nugraha ED, Sato Y, Miura T, Hosoda M, Syaifudin M, Tokonami S and Kashiwakura I: Serum Proteomic and Oxidative Modification Profiling in Mice Exposed to Total Body X-Irradiation. *Antioxidants (Basel)* (2022) 11: 1710.
- Yi L, Hu N, Yin J, Sun J, Mu H, Dai K and Ding D: Up-regulation of calreticulin in mouse liver tissues after long-term irradiation with low-dose-rate gamma rays. *PLoS ONE* (2017) 12: e0182671.
- Chaze T, Hornez L, Chambon C, Haddad I, Vinh J, Peyrat JP, Benderitter M and Guipaud O: Serum Proteome Analysis for Profiling Predictive Protein Markers Associated with the Severity of Skin Lesions Induced by Ionizing Radiation. *Proteomes* (2013) 1: 40–69.
- Guipaud O and Benderitter M: Protein biomarkers for radiation exposure: towards a proteomic approach as a new investigation tool. *Ann Ist Super Sanita* (2009) 45: 278–286.
- Guipaud O: Serum and plasma proteomics and its possible use as detector and predictor of radiation diseases. *Adv Exp Med Biol* (2013) 990: 61–86.
- Helmig S, Lochnit G and Schneider J: Comparative proteomic analysis in serum of former uranium miners with and without radon induced squamous lung cancer. *J Occup Med Toxicol* (2019) 14: 9.
- Autsavapromporn N, Dukaew N, Wongnoppavich A, Chewaskulyong B, Roytrakul S, Klunklin P, Phantawong K, Chitapanarux I, Sripun P, Kritsanuwat R, Amphol S, Pornnumpa C, Suzuki T, Kudo H, Hosoda M and Tokonami S: IDENTIFICATION OF NOVEL BIOMARKERS FOR LUNG CANCER RISK IN HIGH LEVELS OF RADON BY PROTEOMICS: A PILOT STUDY. *Radiat Prot Dosimetry* (2019) 184: 496–499.
- Xu NY, Zhang SP, Nie JH, Li JX and Tong J: Radon-induced proteomic profile of lung tissue in rats. *J Toxicol Environ Health A* (2008) 71: 361–366.
- Xu NY, Zhang SP, Dong L, Nie JH and Tong J: Proteomic Analysis of Lung Tissue of Rats Exposed to Cigarette Smoke and Radon. *J Toxicol Environ Health A* (2009) 72: 752–758.
- Kataoka T, Kanzaki N, Sakoda A, Shuto H, Yano J, Naoe S, Tanaka H, Hanamoto K, Terato H, Mitsunobu F and Yamaoka K: Evaluation of the redox state in mouse organs following radon inhalation. *J Radiat Res* (2021) 62: 206–216.
- Kataoka T, Shuto H, Yano J, Naoe S, Ishida T, Nakada T, Yamato K, Hanamoto K, Nomura T and Yamaoka K: X-Irradiation at 0.5 Gy after the forced swim test reduces forced swimming-induced immobility in mice. *J Radiat Res* (2020) 61: 517–523.
- Faienza MF, Francavilla R, Goffredo R, Ventura A, Marzano F, Panzarino G, Marinelli G, Cavallo L and Di Bitonto G: Oxidative stress in obesity and metabolic syndrome in children and adolescents. *Horm Res Paediatr* (2012) 78: 158–164.
- Chong J and Xia J: MetaboAnalystR: an R package for flexible and reproducible analysis of metabolomics data. *Bioinformatics* (2018) 34: 4313–4314.
- Bautista JR, Pavlakis A and Rajagopal A: Bayesian analysis of randomized controlled trials. *Int J Eat Disord* (2018) 51: 637–646.
- Bijlsma S, Bobeldijk I, Verheij ER, Ramaker R, Kochhar S, Macdonald IA, van Ommen B and Smilde AK: Large-scale human metabolomics studies: a strategy for data (pre-) processing and validation. *Anal Chem* (2006) 78: 567–574.
- Lucia FC and Gottfried JL: Rapid analysis of energetic and geo-materials using LIBS. *Mater Today* (2011) 14: 274–281.
- Chamrad DC, Körting G, Stühler K, Meyer HE, Klose J and Blüggel M: Evaluation of algorithms for protein identification from sequence databases using mass spectrometry data. *Proteomics* (2004) 4: 619–628.
- Thiede B, Höhenwarter W, Krah A, Mattow J, Schmid M, Schmidt F and Jungblut PR: Peptide mass fingerprinting. *Methods* (2005) 35: 237–247.
- Ahrné E, Müller M and Lisacek F: Unrestricted identification of modified proteins using MS/MS. *Proteomics* (2010) 10: 671–686.
- Wang G, Wu WW, Zhang Z, Masilamani S and Shen RF: Decoy methods for assessing false positives and false discovery rates in

- shotgun proteomics. *Anal Chem* (2009) 81: 146–159.
29. Levitsky LI, Ivanov MV, Lobas AA and Gorshkov MV: Unbiased False Discovery Rate Estimation for Shotgun Proteomics Based on the Target-Decoy Approach. *J Proteome Res* (2017) 16: 393–397.
 30. Triba MN, Le Moyec L, Amathieu R, Goossens C, Bouchemal N, Nahon P, Rutledge DN and Savarin P: PLS/OPLS models in metabolomics: the impact of permutation of dataset rows on the K-fold cross-validation quality parameters. *Mol BioSyst* (2015) 11: 13–19.
 31. Westerhuis JA, Hoefsloot HCJ, Smit S, Vis DJ, Smilde AK, van Velzen EJJ, van Duijnhoven JPM and van Dorsten FA: Assessment of PLS-DA cross validation. *Metabolomics* (2008) 4: 81–89.
 32. Li S, Liu F, Wu M, Li Y, Song X and Yin J: Effects of Drying Treatments on Nutritional Compositions, Volatile Flavor Compounds, and Bioactive Substances of Broad Beans. *Foods* (2023) 12: 2160.
 33. Yamaoka K and Kataoka T: Confirmation of efficacy, elucidation of mechanism, and new search for indications of radon therapy. *J Clin Biochem Nutr* (2022) 70: 87–92.
 34. Stadtman ER, Van Remmen H, Richardson A, Wehr NB and Levine RL: Methionine oxidation and aging. *Biochim Biophys Acta* (2005) 1703: 135–140.
 35. Xia J, Broadhurst DI, Wilson M and Wishart DS: Translational biomarker discovery in clinical metabolomics: an introductory tutorial. *Metabolomics* (2013) 9: 280–299.
 36. Joseph NF, Swarnkar S and Puthanveetil SV: Double Duty: Mitotic Kinesins and Their Post-Mitotic Functions in Neurons. *Cells* (2021) 10: 136.
 37. Xiao Q, Hu X, Wei Z and Tam KY: Cytoskeleton Molecular Motors: Structures and Their Functions in Neuron. *Int J Biol Sci* (2016) 12: 1083–1092.
 38. Schiavo G, Greensmith L, Hafezparast M and Fisher EM: Cytoplasmic dynein heavy chain: the servant of many masters. *Trends Neurosci* (2013) 36: 641–651.
 39. Hertz L and Rothman DL: Glutamine-Glutamate Cycle Flux Is Similar in Cultured Astrocytes and Brain and Both Glutamate Production and Oxidation Are Mainly Catalyzed by Aspartate Aminotransferase. *Biology (Basel)* (2017) 6: 17.
 40. Cooper AJ and Jeitner TM: Central Role of Glutamate Metabolism in the Maintenance of Nitrogen Homeostasis in Normal and Hyperammonemic Brain. *Biomolecules* (2016) 6: 16.
 41. Kim K, Lee SG, Kegelman TP, Su ZZ, Das SK, Dash R, Dasgupta S, Barral PM, Hedvat M, Diaz P, Reed JC, Stebbins JL, Pellecchia M, Sarkar D and Fisher PB: Role of excitatory amino acid transporter-2 (EAAT2) and glutamate in neurodegeneration: opportunities for developing novel therapeutics. *J Cell Physiol* (2011) 226: 2484–2493.
 42. Yenari MA, Liu J, Zheng Z, Vexler ZS, Lee JE and Giffard RG: Antiapoptotic and anti-inflammatory mechanisms of heat-shock protein protection. *Ann N Y Acad Sci* (2005) 1053: 74–83.
 43. Goodman SC, Letra A, Dorn S, Araujo-Pires AC, Vieira AE, Chaves de Souza L, Yadlapati M, Garlet GP and Silva RM: Expression of heat shock proteins in periapical granulomas. *J Endod* (2014) 40: 830–836.
 44. Yang Y, Zhang S, Guan J, Jiang Y, Zhang J, Luo L and Sun C: SIRT1 attenuates neuroinflammation by deacetylating HSPA4 in a mouse model of Parkinson's disease. *Biochim Biophys Acta Mol Basis Dis* (2022) 1868: 166365.
 45. Harauz G, Ladizhansky V and Boggs JM: Structural polymorphism and multifunctionality of myelin basic protein. *Biochemistry* (2009) 48: 8094–8104.
 46. Müller C, Bauer NM, Schäfer I and White R: Making myelin basic protein -from mRNA transport to localized translation. *Front Cell Neurosci* (2013) 7: 169.
 47. Heymann JA and Hinshaw JE: Dynamins at a glance. *J Cell Sci* (2009) 122: 3427–3431.
 48. Fà M, Staniszewski A, Saeed F, Francis YI and Arancio O: Dynamin 1 Is Required for Memory Formation. *PLoS ONE* (2014) 9: e91954.
 49. Matsubara K, Kuki I, Ishioka R, Yamada N, Fukuoka M, Inoue T, Nukui M, Okamoto N, Mizuguchi T, Matsumoto N and Okazaki S: Abnormal axonal development and severe epileptic phenotype in Dynamin-1 (DNM1) encephalopathy. *Epileptic Disord* (2024) 26: 139–143.
 50. Jebelli J, Hamper MC, Van Quelef D, Caraballo D, Hartmann J and Kumi-Diaka J: The Potential Therapeutic Effects of Low-Dose Ionizing Radiation in Alzheimer's Disease. *Cureus* (2022) 14: e23461.
 51. Nikolaisvili M, Nanobashvili Z, Mitagvaria N, Chkadua G, Bilanishvili I, Nozadze E, Jikia G, Museliani T and Dondoladze K: EFFECTS OF INHALATION OF LOW DOSES OF RADON IN THE KRUSHINSKY-MOLODKINA RAT STRAIN AND STUDY OF VARIOUS BEHAVIORAL CHARACTERISTICS. *JECM (Experimental and Clinical Medicine Georgia)* (2023) No. 3.
 52. Kataoka T, Sakoda A, Ishimori Y, Toyota T, Nishiyama Y, Tanaka H, Mitsunobu F and Yamaoka K: Study of the response of superoxide dismutase in mouse organs to radon using a new large-scale facility for exposing small animals to radon. *J Radiat Res* (2011) 52: 775–781.
 53. Sakoda A, Ishimori Y, Kawabe A, Kataoka T, Hanamoto K and Yamaoka K: Physiologically Based Pharmacokinetic Modeling of Inhaled Radon to Calculate Absorbed Doses in Mice, Rats, and Humans. *J Nucl Sci Technol* (2010) 47: 731–738.
 54. Silva JC, Gorenstein MV, Li GZ, Vissers JP and Geromanos SJ: Absolute quantification of proteins by LCMSE: a virtue of parallel MS acquisition. *Mol Cell Proteomics* (2006) 5: 144–156.